Distinct preplay of multiple novel spatial experiences in the rat

Distinct preplay of multiple novel spatial experiences in the rat

George Dragoi[1] and Susumu Tonegawa[1]

The Picower Institute for Learning and Memory, RIKEN-MIT Center for Neural Circuit Genetics, Department of Biology, and Department of Brain and Cognitive Sciences, Massachusetts Institute of Technology, Cambridge, MA 02139

Contributed by Susumu Tonegawa, April 11, 2013 (sent for review March 4, 2013)

The activity of ensembles of hippocampal place cells represents a hallmark of an animal's spatial experience. The neuronal mechanisms that enable the rapid expression of novel place cell sequences are not entirely understood. Here we report that during sleep or rest, distinct sets of hippocampal temporal sequences in the rat preplay multiple corresponding novel spatial experiences with high specificity. These findings suggest that the place cell sequence of a novel spatial experience is determined, in part, by an online selection of a subset of cellular firing sequences from a larger repertoire of preexisting temporal firing sequences in the hippocampal cellular assembly network that become rapidly bound to the novel experience. We estimate that for the given context, the recorded hippocampal network activity has the capacity to preplay an extended repertoire of at least 15 future spatial experiences of similar distinctiveness and complexity.

It is a matter of debate whether specific sequences of place cells (1) encoding different novel spatial experiences in the rat are formed exclusively during the experiences (2–4) or are, in part, preconfigured in the form of correlated temporal sequences that are expressed before the experience (5–7). Previous work in mice has shown that in the naïve animal, temporal firing sequences expressed in association with sharp-wave ripples during sleep or rest can preplay future spatial sequences of place cells encoding novel environments (5). However, it remains unclear whether place cell sequences encoding a novel spatial experience are preconfigured as a dominant cluster of temporal sequences preferentially preplaying the subsequent experience or whether they are selected from an existing larger repertoire of temporally organized sequences. The latter would confer the hippocampal network with the capacity to rapidly encode multiple parallel spatial experiences, but the extent of this capacity has not been addressed experimentally. Here we investigate these two issues.

Results

Preplay of Future Place Cell Sequences and Spatial Trajectories. Ensembles of place cells were recorded from the CA1 area of the hippocampus in three experimentally naïve rats during sleep/rest sessions and during subsequent first-time exploration of 1.5-m–long linear tracks (Fig. 1*A*). The sleep/rest sessions were conducted in a sleep/rest box surrounded by high opaque walls that blocked the rats' view of the room except for a limited portion of the ceiling. After the naïve rats went through an ∼1-h sleep/rest period, a linear track (*Materials and Methods*) was introduced into the room for the first time. Place cell sequence templates were computed by ordering the place cells based on the location of their place field peak firing during exploration of the linear track (Fig. 1*B*, *Right*). Spiking events were detected during sleep/rest frames (8) as epochs of multiunit activity recorded from at least six different pyramidal cells with a <100-ms interspike interval in the multiunit activity, flanked by epochs of >100 ms of silence (4, 5, 9). For each spiking event, the order of cells firing during sleep/rest (temporal sequence) was correlated with the order in which they subsequently fired as place cells during exploration of the linear track (spatial sequence) (2, 4, 5, 9). During an event, if a cell fired more than one spike, only the first spike was further considered to calculate the "temporal" sequence of neuronal firing (2, 8, 9). Similar results (Fig. S1) were obtained when individual cell firing rates were accounted for by considering all of the spikes emitted during the events (4, 10). An event was considered as preplay of the future place cell sequence (Fig. 1*B*, *Left*) when the absolute value of the corresponding temporal–spatial correlation exceeded the 97.5 percentile of a distribution of absolute correlation values calculated between the event and 500 surrogate spatial sequences created by shuffling the original spatial order of place cells (5).

We used a Bayesian reconstruction algorithm (5, 11, 12) to decode the rat's position from the neuronal activity recorded during the first run session on the novel track or during the preceding sleep/rest session in the box. The decoded (reconstructed) position during the run was compared with the actual trajectory of the animal (Fig. 1*C*). The cumulative error (Fig. 1*D*, red lines) and average error (Fig. 1*E*, red lines) of the reconstructed position were significantly smaller than the distribution of errors obtained by shuffling for 500 times the time bins (Fig. 1 *D* and *E*, *Left*) or position bins (Fig. 1 *D* and *E*) of the original reconstructed position of the animal during the run. Moreover, in a significant number of cases, the firing rate-based Bayesian decoding of the neuronal activity of "all" spikes during each spiking event detected as above during sleep/rest revealed patterns of activation of place cells subsequently coding spatial trajectories on the novel linear track that was only later explored for the first time (Fig. 1*F*). For each event, the decoded trajectory during the preceding sleep/rest was significant if the original score for the line fitting along the trajectory (5, 12) exceeded the 99th percentile of each of the two distributions of 500 scores ($P < 0.01$; Fig. 1*F*). These scores were calculated by fitting a line through the surrogate probability distributions of positions (12) (*Materials and Methods*) obtained by shuffling the time bins or position bins of the original probability distribution function decoded during the sleep/rest session (5, 12).

Statistical Significance of Preplay of Single Novel Spatial Experience. Of all the detected spiking events during sleep/rest in the three rats, 9.8% were classified as significant preplay of the future spatial sequences because they were significantly correlated with place cell sequences expressed during the first-time exploration of the novel track. Preplay sequences spanned 82.6% of the track length on average ($n = 1{,}388$; $P < 10^{-200}$, binomial probability test; Fig. 1*G* and Fig. S2). They occurred in the forward or reverse order (forward:reverse ratio = 1.04) and generally were significantly correlated specifically with place cell sequences of one direction of movement (85.3% of preplay sequences were

Author contributions: G.D. and S.T. designed research; G.D. performed research; G.D. analyzed data; and G.D. and S.T. wrote the paper.

The authors declare no conflict of interest.

Freely available online through the PNAS open access option.

[1]To whom correspondence may be addressed. E-mail: gdragoi@mit.edu or tonegawa@mit.edu.

This article contains supporting information online at www.pnas.org/lookup/suppl/doi:10.1073/pnas.1306031110/-/DCSupplemental.

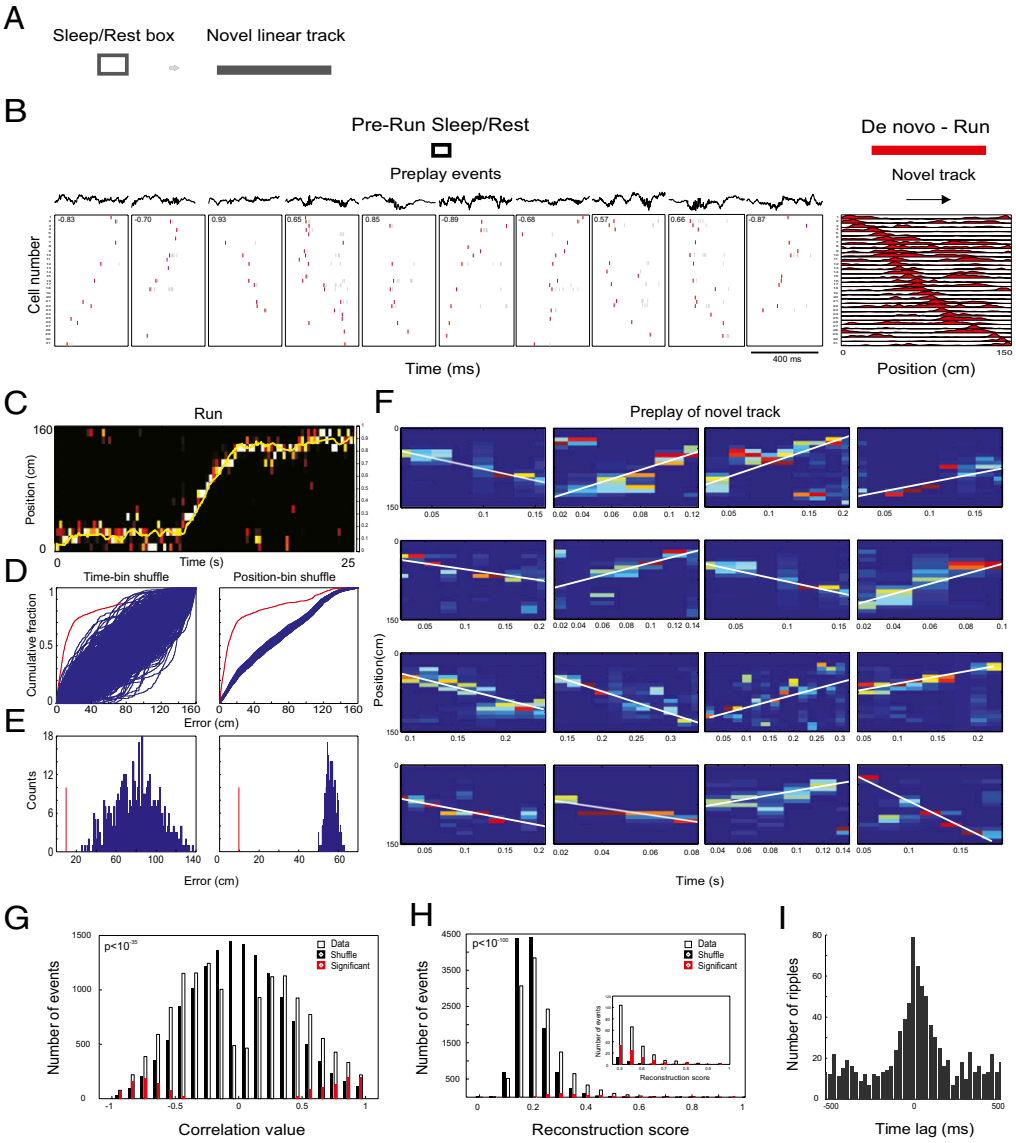

Fig. 1. Preplay of future place cell sequences and spatial trajectories during sleep/rest in the naïve rat. (*A*) Schematic of the sequence of experimental sessions (one-track experiment). Preplay events were detected during the first sleep/rest session of naïve rats (*Left*) and correlated with the place cell sequences on the linear track (*Right*). (*B*) Examples of preplay spiking events during the sleep/rest session in the sleep box preceding the first run on the novel linear track (first 10 boxes; *Left*) and the corresponding place cell sequence during the run (*Right*) in one naïve rat. Tick marks (first 10 boxes; *Left*) indicate individual spikes during preplay events. For each event and for each participating cell, the first spike emitted during the event is represented in red, whereas all of the remaining spikes are in gray. The numbers in the boxes are the correlation values between the temporal order of spiking and the spatial order of activation corresponding to each preplay event. Corresponding local field potential recordings are shown above the spiking events. The horizontal arrow (*Right*) indicates the order of the place cell activation during the run. (*C*) Bayesian decoding of the rat's position from the spiking activity of all cells during one lap run on the novel track (250-ms bins, animal velocity >10 cm/s). The heat map represents the decoded position of the animal, whereas the yellow line displays its actual position on the track. (*D*) Cumulative probability distribution of the error of the Bayesian decoding of the rat's position (red curves) compared with the distribution of errors of 500 shuffles (blue curves) of time bins (*Left*) and position bins (*Right*). (*E*) Average error of the Bayesian decoding of the rat's position (red lines; scaled up 10 times) compared with the distribution of average errors of 500 shuffles (blue curves) of time bins (*Left*) and position bins (*Right*). (*F*) Examples of significant decoding of a future trajectory on the novel track from ensemble place cell activity during the sleep/rest session before novel track exploration (i.e., prerun sleep/rest) in one naïve rat (20-ms bins, animal velocity <1 cm/s). The white lines show the linear fit maximizing the likelihood along the virtual trajectory. (*G*) Distribution of correlation values between spiking events and the place cell sequence for all events occurring during the prerun sleep/rest in three animals. Open bars, spiking events vs. the original (unshuffled) templates; filled black bars, spiking events vs. 500 shuffled templates scaled down 500 times; red bars, distribution of preplay (i.e., significant) events. The *P* value reflects the minimum significance level (i.e., the largest *P* value) of the difference between the original set (open bars) and any of the 500 sets of shuffled (black bars) correlation values using the rank-sum test. (*H*) Distribution of decoding scores for the virtual novel track trajectory for all events occurring during the prerun sleep/rest in three rats. Open bars, scores during all spiking events; filled black bars, scores of 500 time-bin shuffles scaled down 500 times; red bars, scores of significant events exceeding the 99th percentile of both time-bin and position-bin shuffle distributions. The *P* value reflects the minimum significance level (i.e., the largest *P* value) of the difference between the original set (open bars) and any of the 500 sets of shuffled (black bars) scores using the rank-sum test. (*Inset*) Enlarged display of the distribution for score values between 0.5 and 1. (*I*) Cross-correlation between preplay events and ripple occurrence in CA1 during prerun sleep/rest in the three rats (the distribution of the time of ripple occurrence with reference to the time of occurrence of the significant preplay events).

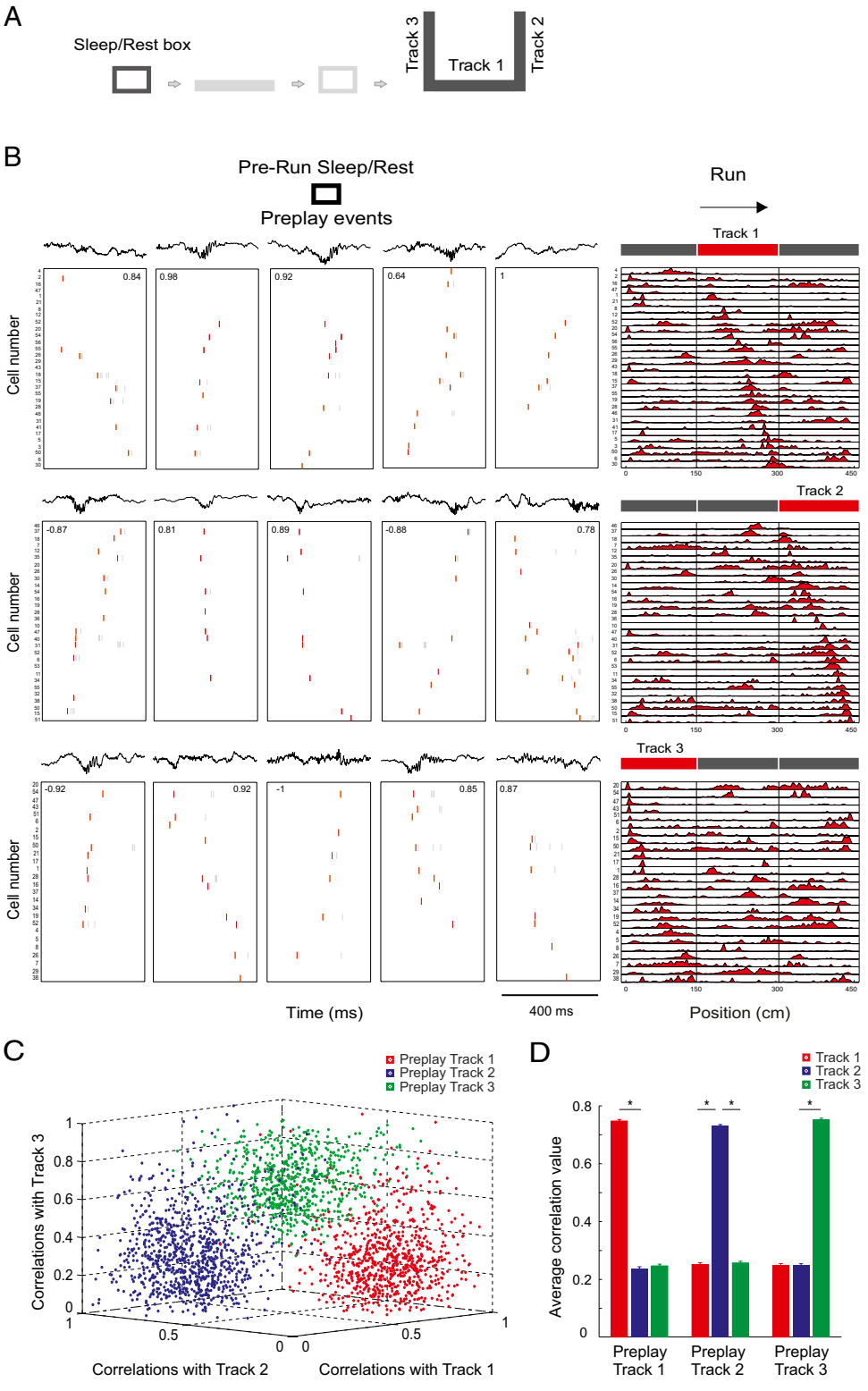

Fig. 2. Selection of specific hippocampal temporal sequences during encoding of multiple novel spatial experiences in the rat. (*A*) Schematic showing the sequence of experimental sessions (three-track experiment). All preplay events were detected from the first sleep/rest session of naïve rats (black box) and correlated with the place cell sequences from the three tracks (U-shape maze). Animals were familiarized with track 1 (run and sleep/rest sessions depicted in light gray) before the exploration of the U-shape maze, whereas tracks 2 and 3 remained novel. (*B*) Examples of preplay (*Left*) of three distinct future place cell sequences on three linear tracks (*Right*) during sleep/rest in one naïve rat. For each track, the format display is the same as in Fig. 1*B*. Activity corresponding to tracks 1, 2, and 3 is in the *Top*, *Middle*, and *Bottom*, respectively. For comparison, the place cell activity on the other two tracks is presented adjacent to the place cell sequences corresponding to tracks 1 (*Top*), 2 (*Middle*), and 3 (*Bottom*). The U-shaped track has been linearized for easier display. (*C*) Three-dimensional scatterplot of absolute correlation values between spatial templates of the three novel tracks and preplay events that are significantly correlated with only one novel track. Red, blue, and green dots, events that preplay track 1 only, track 2 only, and track 3 only, respectively. Note the presence of three well-isolated clusters corresponding to preplay events, indicating specific correlations with each of the three novel tracks. (*D*) Average absolute correlation values between spatial templates of the three novel tracks and preplay events specific to one novel linear track. The *Left*, *Center*, and *Right* groups of three bars correspond to the red, blue, and green points from *C*, respectively. Stars represent significant differences between groups determined using the paired *t* test. Error bars are standard error of the mean.

unidirectional; mean absolute correlations with the preferred vs. unpreferred direction templates, 0.78 vs. 0.44, $P < 10^{-141}$, rank-sum test). The peak of the distribution of absolute correlation values of all events with the novel track (Fig. 1*G*) is around 0.25. This indicates that whereas some events have no correlation with the future experience ($r \sim 0$; Fig. 1*G*), most of the temporal sequences in the naïve rats are not completely independent from the future place cell sequence activity on the linear track, despite only a minority of them reaching significance (Fig. 1*G*). This residual correlation could be due to the organization of neurons in cellular assemblies based on nonstructured past experiences in similar contexts. In addition, in 4% of the spiking events, decoding revealed significant spatial trajectories on the novel linear track that spanned 42.2% of the track length on average

($n = 502$, $P < 10^{-143}$, binomial probability test; Fig. 1*H* and Fig. S3; *Materials and Methods*). The incidence of significant decoded trajectories that exceeded the 97.5 percentile of each of the two distributions of 500 shuffle scores ($P < 0.025$) was over 7.3% ($n = 919$, $P < 10^{-174}$, binomial probability test). The significant preplay events occurred in association with ripple oscillations (Fig. 1*I*), and the spatial sequences were compressed in time (Fig. 1*B*, *Left*) and were preplayed at an average speed of 4.9 m/s, about 20 times faster than the running speed of the rats (average 25 cm/s).

Distinct Preplay of Multiple Novel Spatial Experiences. The existence of a significant set of correlated preplay events indicates that the internal dynamics of the hippocampal network contribute to the online expression of the very next place cell sequence. However, it remains unclear whether the remaining set of uncorrelated temporal sequences reflects noisy brain states or rather reflects internal organization of neurons in sequential cell assemblies (13) that could result in additional preplay sequences of yet to be performed spatial experiences. To test whether, in the naïve rat, given temporal sequences during sleep/rest preplay in parallel multiple potential novel spatial experiences, the naïve animals were exposed within 1 d to three contiguous novel linear tracks that were each 1.5-m–long and attached in a U shape (Fig. 2*A*; *Materials and Methods*). The rats were first exposed to track 1; later they accessed each of the two parallel tracks (tracks 2 and 3) (Fig. 2*A*) by explicitly exiting track 1 and turning 90° at corner locations where tracks 2 and 3 were previously separated by barriers from track 1. A unique sequence of place cells encoded each of the three tracks with high specificity (Fig. 2*B*). Using the above criteria for significance, each of the three tracks had significantly matching temporal sequences that could be recorded several hours earlier during the sleep/rest session in the naïve state, before the rats had "any" access to the linear tracks. Independent clusters of spiking events (Fig. 2*C*) were highly correlated specifically with only one track ($P < 10^{-200}$, paired t test; corresponding tracks, $r > 0.73$ vs. noncorresponding tracks, $r < 0.26$, for tracks 1–3; Fig. 2*D*), and all tracks had equally strong correlation values with the corresponding cluster of preplay events (mean of absolute correlations, $r > 0.73$ for each track; Fig. 2*D*).

A similar proportion of temporal sequences out of all detected spiking events significantly correlated exclusively with one track but not the other two (6.65%, 6.8%, and 6.76% events specifically preplayed tracks 1, 2, and 3, respectively; Fig. 3*A*, *Upper* and Fig. S4). Overall, preplay sequences displayed high specificity (>90% track specificity on any pair of tracks; Fig. 3*A*, *Lower* and Fig. S4) and little overall overlap across tracks (1.5% of all events correlated with more than one track; Fig. 3*A* and Fig. S4). In contrast, 93.7% of individual place cells were active in more than one track in at least one direction (Fig. 3*B*), suggesting that in the CA1 area, the basic unit that specifically represents different novel spatial experiences is the sequence of place cell firing rather than the identity of individual cells. Overall, these findings indicate that neurons in hippocampal area CA1 are organized during sleep/rest by default into distinct sequential cellular assemblies in the temporal domain (Fig. 3*B*, colored lines) that can rapidly, simultaneously, and specifically encode multiple future novel spatial experiences (note that the arrows in Fig. 3*B* do not indicate synaptic connections of CA1 cells, just the order in which they fire).

Estimation of the Hippocampal Network Capacity for Preplay. We speculate that the remaining uncorrelated events comprising 78% of all of the detected events during sleep/rest in the naïve state have the potential to preplay additional distinct future novel spatial experiences (Fig. 3*B*, gray lines). To estimate the capacity of the hippocampal network to preplay novel spatial experiences during the sleep/rest session in the naïve state, we took into account the relationship that exists in our data between the number of novel linear tracks explored by our animals and the proportion of highly specific preplay sequences that we detected

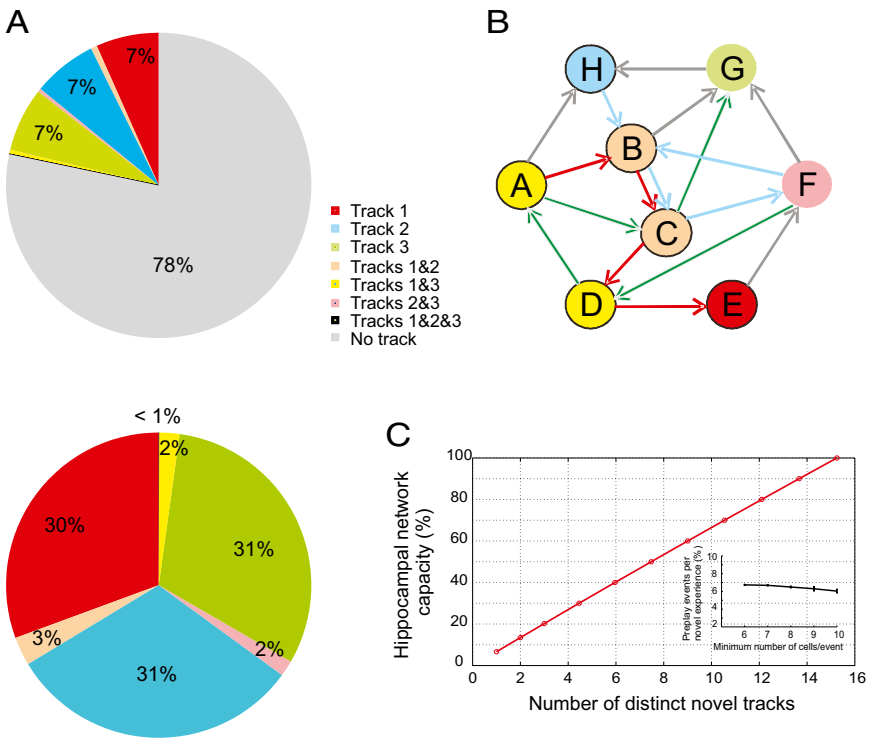

Fig. 3. Quantification and further estimation of the capacity of the hippocampal network during sleep/rest to preplay multiple novel experiences. (*A*) Proportion of preplay events significantly correlated with at least one track (see legend for color code) out of all detected spiking events (*Upper*) and all significant preplay events (*Lower*) during sleep/rest in the naïve rat from Fig. 2 (n = 9,835 total events). (*B*) Cartoon model of functional connectivity of hippocampal cellular assemblies corresponding to the three tracks. Each circled letter corresponds to an individual cell; arrows do not indicate synaptic connections of CA1 cells but rather the order of cell firing in CA1 as a result of anatomical connectivity with the upstream CA3, in which pyramidal cells are efficiently connected by recurrent circuits. Arrows are color-coded (track 1, red, sequence A→B→C→D→E; track 2, blue, F→D→A→C→G; track 3, green, H→B→C→F→B; no track, gray). Individual cells are color-coded according to their participation in encoding individual tracks as in *A*. (*C*) Estimation of the number of novel linear tracks the hippocampal network can preplay in a given sleep/rest session. The red curve displays a polynomial extrapolation of the first three data points (1–3 on the abscissa) that represent the percentage of preplay events out of the total number of spiking events that significantly correlated with one track (e.g., track 1), two tracks (e.g., track 1 or track 2), and three tracks (e.g., track 1, track 2, or track 3), respectively, as described in *A*. (*Inset*) Mean percentage of preplay events per novel linear track as a function of the minimum number of cells required to be simultaneously active during a spiking event. Error bars are SEM.

during sleep/rest. We modeled this relationship as a polynomial function to extrapolate the number of potential novel tracks that could be preplayed by individual subsets of temporal sequences from the larger repertoire expressed during sleep/rest that would be specifically correlated with only one track (Fig. 3*C*). We estimate that during a given sleep/rest session, the hippocampal network of the recorded neurons has the capacity to preplay with high specificity at least 15 distinct novel tracks of similar distinctiveness (>90% temporal sequence specificity on a pair of tracks) and level of complexity (Fig. 3*C*). The average proportion of preplay events per novel track, and implicitly our estimate of network capacity, does not change significantly when the minimum number of cells simultaneously active during a spiking event changes from 6 to 10 ($P > 0.05$, rank-sum test; Fig. 3*C*, *Inset*).

Discussion

Our findings show that the specificity of the representation of a particular novel spatial experience in the rat is achieved during the experience via the "selection" of subsets of corresponding temporal sequences from a larger repertoire of preconfigured temporal sequences rather than from a dominant cluster of temporal sequences preplaying the very next experience (5). The corresponding temporal firing sequences are rapidly bound to the specific novel experiences in the form of specific place cell sequences. The selection of specific sequences from a larger preconfigured repertoire confers the hippocampal network with the capacity to rapidly encode multiple parallel novel experiences. The preplay events described in our study were recorded exclusively in the sleep/rest box with high opaque walls during the sleep/rest session before the linear tracks were first introduced into the room. We can thus exclude the possibility that during these events the animals "mentally traveled" within the room, having view of the linear tracks. Moreover, the fact that more than 90% of all the recorded CA1 place cells are active on more than one track indicates that individual CA1 cells participate in multiple cellular assemblies encoding different spatial experiences and that individually they cannot accurately distinguish the identity of multiple linear tracks. Instead, the sequences of CA1 place cells in our data accurately distinguish across multiple linear tracks. Given that the subsets of preplay sequences devoted to the representation of each of the three tracks represent 6–7% of all detected spiking events with similar proportions across tracks, we estimate that for a similar experimental setting and based on the activity of the same group of CA1 neurons, the hippocampal network has the capacity to simultaneously encode at least 15 different novel spatial experiences of similar distinctiveness and complexity. These estimates are based on an average of 6–7% of all temporal sequences preplaying each track and ~90% novel track specificity between pairs of tracks. If a smaller proportion of events preplays each track or if a greater overlap is tolerated for the distinction of a pair of experiences, then the total encoding repertoire of the hippocampal network will be greater. Similarly, if the activity of all of the hippocampal cells were to be taken into account in multiple contexts (14), the hippocampal capacity to encode different novel experiences would be expected to be higher. The capacity of the hippocampal network for a rich repertoire of temporal preplay sequences may contribute to the role of the hippocampus in prospective coding (15), rapid learning (16), and imagining (17, 18).

Materials and Methods

Surgery and Experimental Design. Electrophysiological recordings were performed on three adult Long–Evans male rats. All animals were implanted under isoflurane anesthesia with either 22 independently movable tetrodes (rats 1 and 3) or 64-channel 8-shank NeuroNexus linear silicone octatrodes (rat 2) aiming for area CA1 of the right hippocampus (4 mm postbregma, 1.5–3 mm lateral to midline). The reference electrode was implanted posterior to lambda over the cerebellum. During the following week of recovery, the electrodes were advanced daily while animals rested in a high-wall opaque sleeping box [30 × 45 × 40 (h)-cm]. The animal's position was monitored via two infrared diodes attached to the headstage.

The experimental apparatus consisted of a 150 × 150-cm rectangular elevated linear track maze. All tracks were 6.25-cm–wide and 50 cm above the floor. Experimental sessions were conducted while the animals explored for chocolate sprinkle rewards placed always at the ends of the corresponding linear tracks (one sprinkle at each end of the track on each lap). Neuronal activity was recorded in naïve animals during the prerun sleep/rest session in the sleep box for ~1 h, after which the linear maze was brought into the room and installed, followed by the recording of an additional ~1 h of sleep/rest. Subsequently, the animals were transferred onto the linear maze for the first time and allowed to explore a 150-cm–long linear track whose ends were blocked by 20-cm–high, 10-cm–wide barriers (track 1). The animals were familiarized with the linear track via repeated run–sleep/rest sessions. Finally, while the animals were on the linear track, the two end barriers were lifted, allowing the animals to explore for the first time two additional 150-cm–long linear tracks attached to the ends of track 1 (tracks 2 and 3) to form the shape of the letter "U." After completion of all experiments, the brains of all the rats were perfused, fixed, sectioned, and stained using cresyl violet for electrode track reconstruction. The rats were kept on a 12-h light/dark cycle and cared for in accordance with the standards of the Massachusetts Institute of Technology Committee on Animal Care and in compliance with National Institutes of Health guidelines.

Recordings and Single-Unit Analysis. A total of 114 neurons were recorded from hippocampal area CA1 in the three rats (31, 27, and 56 neurons) during the sleep/rest and run sessions. Single cells were identified and isolated using the manual clustering method Xclust (19). Pyramidal cells were distinguished from interneurons based on spike width, average rate, and autocorrelations (20).

Place fields were computed as the ratio between the number of spikes and the time spent in 2-cm bins along the track, smoothed with a Gaussian kernel with an SD of 2 cm. Bins where the animal spent a total of less than 0.1 s and periods during which the animal's velocity was below 5 cm/s were excluded. Place field length and peak rate were calculated after separating the direction of movement and linearizing the trajectory of the animal. Linearized place fields were defined as areas with a localized increase in firing rate above 1 Hz for at least five contiguous bins (10 cm). The place field peak rate and location were given by the rate and location of the bin with the highest ratio between spike counts and time spent. Place field borders were defined as the points where the firing rate became less than 10% of the peak firing rate or 1 Hz (whichever was bigger) for at least 2 cm.

Local Field Potential Analysis. Ripple oscillations were detected during sleep/rest periods in the sleep box. The EEG signal was filtered (120–200 Hz) and the ripple-band amplitude was computed using the Hilbert transform. Ripple epochs with maximal amplitude higher than 4 SDs above the mean, beginning and ending at 1 SD, were detected. The time of ripple occurrence (Fig. 1*I*) was the time of its maximal amplitude.

Preplay Analyses Using Template-Matching Procedure. To analyze the preplay process, spiking events were detected during prerun sleep/rest periods in the sleep box (velocity <1 cm/s). Only the spiking events detected in the sleep/rest session before the naïve animals first ran on track 1 were used throughout this study. A spiking event was defined as a transient increase in the multiunit firing activity of a population of at least six different pyramidal cells within a temporal window preceded and followed by at least 100 ms of silence that delimited the beginning and end of the event. The spikes of all the place cells active on the novel track that were emitted during the prerun sleep in the box were sorted by time and further used for the detection of the spiking events. All three naïve animals exhibited a significant number of spiking events in the prerun sleep/rest session. The time of the spiking events used to compute the cross-correlation with the ripple epoch occurrence (Fig. 1*I*) was the average time of all spikes composing the individual spiking events. Place cell sequences (templates) were calculated for each direction of the animal's movement and for each run session for each track by ordering the spatial location of the place field peaks that corresponded to the peak firing rate for each cell above 1 Hz on that track. In the three-track maze design, the spiking events were detected during sleep/rest using the spiking activity of all of the recorded CA1 pyramidal cells regardless of them later becoming place cells on the linear tracks or not. For place cells with fields above 1 Hz on more than one track, only the place field corresponding to the peak firing rate of the place cell on a particular track was considered for the construction of the template of that particular track; individual cells

could participate in the construction of templates of the other tracks. Statistical significance was calculated for each event by comparing the rank-order correlation between the sequence of cell firing in the event (i.e., event sequence) and the place cell sequence (template) on one hand, and the distribution of correlation values between the event sequence and 500 surrogate templates obtained by shuffling the order of place cells on the other (Fig. 1*G*). The significance level was set at 0.025 to control for multiple comparisons (two directions of the run). The proportions of significant preplay events were calculated as the ratio between the number of significant events and the total number of spiking events in which at least six pyramidal cells were active.

The overall significance of the preplay (Fig. 1 *G* and *H*) was calculated by comparing the set of absolute correlation values (and scores) of all events relative to the original template with each of the 500 sets of absolute correlation values (and scores) relative to the shuffled surrogate templates using the rank-sum test.

Bayesian Decoding of Spatial Trajectories. For each cell, we calculated a linearized spatial tuning curve on the novel track during run sessions. Tuning curves were constructed in 2-cm bins from spikes emitted in both run directions at velocities higher than 5 cm/s, and were smoothed with a Gaussian kernel with an SD of 2 cm. We also detected for each cell all of the spiking activity emitted during the spiking events detected during prerun sleep/rest using the rank-order correlation method. We used a Bayesian reconstruction algorithm to decode the position of the animal from the spiking activity during the run (Fig. 1*C*) and during sleep/rest (Fig. 1*F*) in nonoverlapping 250-ms and 20-ms bins, respectively, using the spatial tuning curves (5, 11, 12). The error of the Bayesian decoding during the run was calculated for each time bin as the absolute value of the difference between the spatial position of the maximum decoded probability and the actual position of the animal within that bin. To test for the significance of the decoding during the run, we used two types of shuffles (time bin and position bin) of the original probability distribution of the reconstructed position (PDRP). The shuffling was repeated 500 times for each type. In parallel, we extracted epochs of reconstructed trajectory matching the time of the spiking events as detected using multiunit activity (rank-order correlation method; *Preplay Analyses Using Template-Matching Procedure*). We similarly used two shuffling procedures to measure the quality of the Bayesian decoding during sleep. First, for each event, the original time-bin columns of the PDRP during sleep were replaced with an equal number of time-bin columns randomly extracted from a pool containing the time-bin columns of all PDRPs of all detected events. The shuffling procedure was repeated 500 times. Second, for each event, the position bins of the original PDRP were independently shuffled 500 times. For all original and shuffled PDRPs, a line was fit to the data using a previously described line-finding algorithm (12) that specifies a future linear trajectory on the novel track. The best linear fit was calculated for each event (12) as the preplay score corresponding to the mean estimated likelihood that the animal was on the preplayed trajectory. The scores of lines fitted to the original data were compared with the distributions of scores of shuffled data (12). The trajectory was defined across a set of position estimates during the corresponding epoch (Fig. 1*F*). Only epochs that lasted between 80 ms and 1.2 s and that contained reconstructed trajectories spanning at least 25 cm were considered for further analysis. An epoch was considered significant if the original preplay score exceeded the 99th percentile of both the time-bin and position-bin shuffled distributions of preplay scores.

Estimation of the Network Capacity for Preplay. About 20% of the detected spiking events represented preplay of the three tracks with no overlap across the three tracks (Fig. 3*A*). The remaining ~80% of the sequences were assumed to represent additional capacity of the hippocampal network to represent new tracks in the given context. Because each track specifically correlated with 6–7% of the spiking events, with minimal overlap (a total of an additional 1.5% of events), we estimated how many additional tracks the remaining ~80% of events could preplay.

The function relating the proportion of preplay events to the number of novel linear tracks was calculated based on the three tracks explored (Fig. 3*A*) and was extrapolated using Matlab (MathWorks) as a polynomial (i.e., spline) function (Fig. 3*C*) and as a linear function. The extrapolation used step increases in the proportion of preplay events out of the total number of spiking events detected during sleep/rest for the three tracks to estimate the total number of linear tracks that could be simultaneously and distinctly preplayed in the given spatial context by the remaining ~80% of events. The linear and polynomial extrapolations resulted in similar numbers of linear tracks being estimated. This estimate depends on the proportion of specific preplay events per track and the amount of overlap between pairs of tracks (i.e., preplay specificity) calculated for the range of a minimum of 6–10 cells per event that was common in our datasets. Changes in these parameters will affect the estimate of the network capacity to preplay additional tracks. The total number of recorded neurons will also likely affect these estimates, with more neurons being expected to increase the overall network capacity.

ACKNOWLEDGMENTS. We thank S. P. Layton for comments. This work was supported by National Institutes of Health Grants R01-MH078821 and P50-MH58880 and the RIKEN Brain Science Institute (S.T.).

1. O'Keefe J, Dostrovsky J (1971) The hippocampus as a spatial map. Preliminary evidence from unit activity in the freely-moving rat. *Brain Res* 34(1):171–175.
2. Lee AK, Wilson MA (2002) Memory of sequential experience in the hippocampus during slow wave sleep. *Neuron* 36(6):1183–1194.
3. Kudrimoti HS, Barnes CA, McNaughton BL (1999) Reactivation of hippocampal cell assemblies: Effects of behavioral state, experience, and EEG dynamics. *J Neurosci* 19(10):4090–4101.
4. Foster DJ, Wilson MA (2006) Reverse replay of behavioural sequences in hippocampal place cells during the awake state. *Nature* 440(7084):680–683.
5. Dragoi G, Tonegawa S (2011) Preplay of future place cell sequences by hippocampal cellular assemblies. *Nature* 469(7330):397–401.
6. Samsonovich A, McNaughton BL (1997) Path integration and cognitive mapping in a continuous attractor neural network model. *J Neurosci* 17(15):5900–5920.
7. Dupret D, O'Neill J, Pleydell-Bouverie B, Csicsvari J (2010) The reorganization and reactivation of hippocampal maps predict spatial memory performance. *Nat Neurosci* 13(8):995–1002.
8. Ji D, Wilson MA (2007) Coordinated memory replay in the visual cortex and hippocampus during sleep. *Nat Neurosci* 10(1):100–107.
9. Diba K, Buzsáki G (2007) Forward and reverse hippocampal place-cell sequences during ripples. *Nat Neurosci* 10(10):1241–1242.
10. Gupta AS, van der Meer MA, Touretzky DS, Redish AD (2010) Hippocampal replay is not a simple function of experience. *Neuron* 65(5):695–705.
11. Zhang K, Ginzburg I, McNaughton BL, Sejnowski TJ (1998) Interpreting neuronal population activity by reconstruction: Unified framework with application to hippocampal place cells. *J Neurophysiol* 79(2):1017–1044.
12. Davidson TJ, Kloosterman F, Wilson MA (2009) Hippocampal replay of extended experience. *Neuron* 63(4):497–507.
13. Hebb DO (1949) *The Organization of Behavior: A Neuropsychological Theory* (Wiley, New York).
14. Brown TI, Ross RS, Keller JB, Hasselmo ME, Stern CE (2010) Which way was I going? Contextual retrieval supports the disambiguation of well learned overlapping navigational routes. *J Neurosci* 30(21):7414–7422.
15. Schacter DL, Addis DR, Buckner RL (2008) Episodic simulation of future events: Concepts, data, and applications. *Ann N Y Acad Sci* 1124:39–60.
16. Tse D, et al. (2007) Schemas and memory consolidation. *Science* 316(5821):76–82.
17. Hassabis D, Kumaran D, Vann SD, Maguire EA (2007) Patients with hippocampal amnesia cannot imagine new experiences. *Proc Natl Acad Sci USA* 104(5):1726–1731.
18. Erdem UM, Hasselmo M (2012) A goal-directed spatial navigation model using forward trajectory planning based on grid cells. *Eur J Neurosci* 35(6):916–931.
19. Wilson MA, McNaughton BL (1993) Dynamics of the hippocampal ensemble code for space. *Science* 261(5124):1055–1058.
20. Csicsvari J, Hirase H, Czurkó A, Mamiya A, Buzsáki G (1999) Oscillatory coupling of hippocampal pyramidal cells and interneurons in the behaving rat. *J Neurosci* 19(1):274–287.

Supporting Information

Dragoi and Tonegawa 10.1073/pnas.1306031110

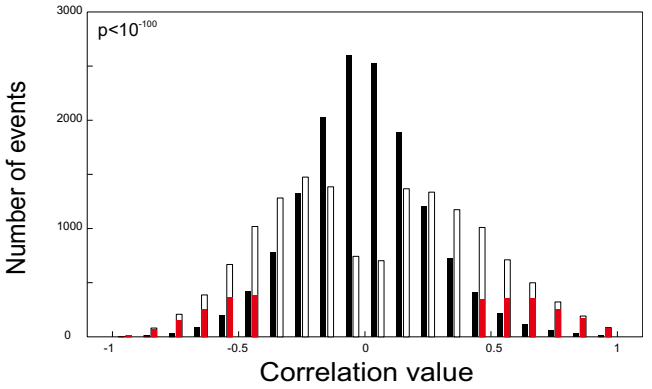

Fig. S1. Quantification of preplay in the rat using all spike analysis. Distribution of correlation values between spiking events and the place cell sequence for all events occurring during the prerun sleep/rest in three animals. For each spike used in the spiking event to compute the correlation, its associated place cell rank order was entered in the place cell sequence. Open bars, spiking events vs. the original (unshuffled) templates; filled black bars, spiking events vs. 500 shuffled templates scaled down 500 times; red bars, distribution of preplay (i.e., significant) events. The *P* value reflects the minimum significance level (i.e., the largest *P* value) of the difference between the original set (open bars) and any of the 500 sets of shuffled (black bars) correlation values using the rank-sum test.

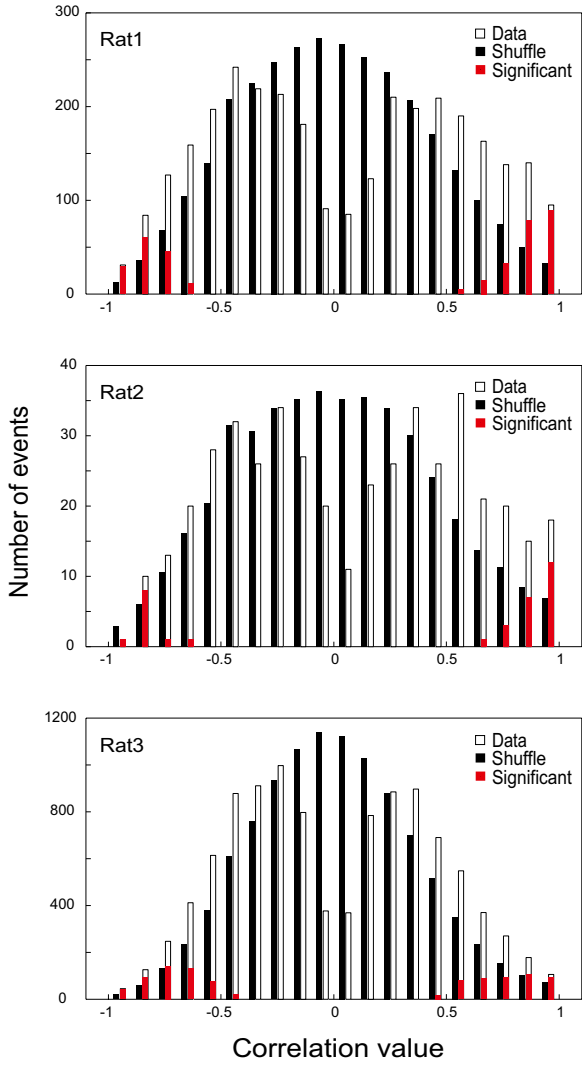

Fig. S2. Quantification of the preplay phenomenon in individual rats. Distribution of correlation values between spiking events and place cell sequence on the novel track for all events occurring during the prerun sleep/rest for rat 1 (*Top*), rat 2 (*Middle*), and rat 3 (*Bottom*). Open bars, spiking events vs. the original (unshuffled) templates; filled bars, spiking events vs. 500 shuffled templates scaled down 500 times; red bars, distribution of preplay (i.e., significant) events. A total of 11.8% of events were significant preplay in rat 1 (368 significant per 3,095 events; $P < 10^{-130}$, binomial probability test), 7.7% in rat 2 (34/441; $P < 10^{-8}$), and 9.3% in rat 3 (986/10,501; $P < 10^{-200}$).

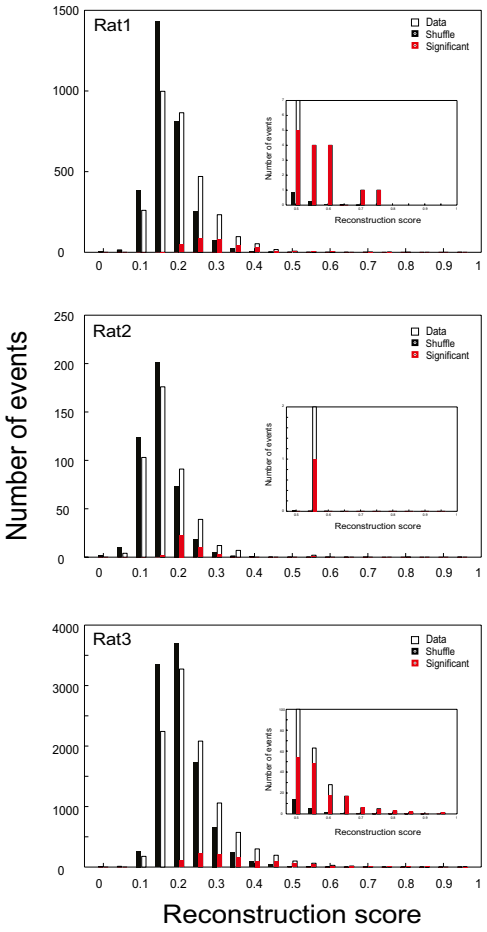

Fig. S3. Quantification of the decoding of future spatial trajectories in individual rats. Distribution of decoding scores for the virtual novel track trajectories for all events occurring during the prerun sleep/rest for rat 1 (*Top*), rat 2 (*Middle*), and rat 3 (*Bottom*). Bars are as in Fig. 1*H*. (*Insets*) Enlarged display of the distribution for corresponding score values between 0.5 and 1. A total of 2.7% (5.4%) of events showed significant decoding of the future trajectories in rat 1 at $P < 0.01$ ($P < 0.025$): 80 (160) significant per 2,945 events, $P < 10^{-14}$ ($P < 10^{-19}$), binomial probability test; 2.3% (5.6%) in rat 2: 10 (24) per 426, $P < 0.008$ ($P < 0.0002$); 4.5% (8%) in rat 3: 412 (735) per 9,159, $P < 10^{-130}$ ($P < 10^{-155}$).

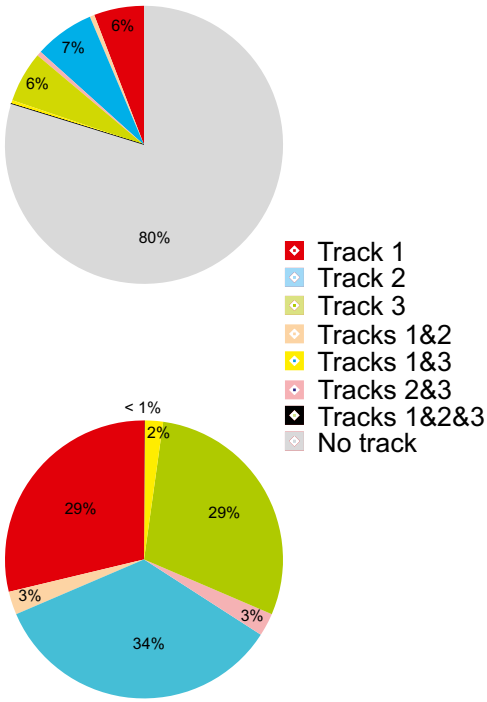

Fig. S4. Proportion of preplay events in the three-track maze. Proportion of preplay events correlated with at least one track (see legend for color code) out of all detected spiking events using all pyramidal cells regardless of their place field activity on the three tracks (*Upper*) and out of all preplay events (*Lower*) detected as above during prerun sleep/rest in the three rats ($n = 768$ events preplaying track 1 only, $n = 920$ events preplaying track 2 only, $n = 781$ events preplaying track 3 only, $n = 72$ events preplaying tracks 1 and 2 only, $n = 71$ events preplaying tracks 2 and 3 only, $n = 56$ events preplaying tracks 1 and 3 only, $n = 3$ events preplaying tracks 1, 2, and 3, $n = 10,517$ events uncorrelated with any of the three tracks).